


Metabolomics analysis of mycelial exudates provides insights into fungal antagonists of *Armillaria*

Jian Zhan[#], Jing Yuan[#], Jianwei Liu, Fengming Zhang, Fuqiang Yu and Yanliang Wang 

The Germplasm Bank of Wild Species, Yunnan Key Laboratory for Fungal Diversity and Green Development, Kunming Institute of Botany, Chinese Academy of Sciences, Kunming, China

ABSTRACT

The genus *Armillaria* has high edible and medical values, with zones of antagonism often occurring when different species are paired in culture on agar media, while the antagonism-induced metabolic alteration remains unclear. Here, the metabolome of mycelial exudates of two Chinese *Armillaria* biological species, C and G, co-cultured or cultured separately was analysed to discover the candidate biomarkers and the key metabolic pathways involved in *Armillaria* antagonists. A total of 2,377 metabolites were identified, mainly organic acids and derivatives, lipids and lipid-like molecules, and organoheterocyclic compounds. There were 248 and 142 differentially expressed metabolites between group C-G and C, C-G, and G, respectively, and fourteen common differentially expressed metabolites including malate, uracil, Leu-Gln-Arg, etc. Metabolic pathways like TCA cycle and pyrimidine metabolism were significantly affected by C-G co-culture. Additionally, 156 new metabolites (largely organic acids and derivatives) including 32 potential antifungal compounds, primarily enriched into biosynthesis of secondary metabolites pathways were identified in C-G co-culture mode. We concluded that malate and uracil could be used as the candidate biomarkers, and TCA cycle and pyrimidine metabolism were the key metabolic pathways involved in *Armillaria* antagonists. The metabolic changes revealed in this study provide insights into the mechanisms underlying fungal antagonists.

ARTICLE HISTORY

Received 25 April 2023
Accepted 15 July 2023

KEYWORDS

antagonists; co-culture;
honey mushroom; LC-MS/MS;
metabolites

1. Introduction


Armillaria (Fr.) Staude, also known as honey mushroom or zhen-mo, belongs to the family of Physalacriaceae (Matheny et al. 2006; Collins et al. 2013). Since the first discovery of *Armillaria* biological species (Korhonen 1978), nearly 40 biological species of *Armillaria* have been identified, mainly distributed in the tropical and temperate forest areas of North America, Europe, and Northeast Asia (He et al. 2019; Zhao et al. 2008). *Armillaria* can be facultatively parasitic or saprophytic on plants and have an indispensable symbiotic relationship with *Gastrodia elata* and *Grifola umbellata*, which are precious Chinese medicinal materials (Yuan et al. 2018). As an edible and medicinal macrofungi, *Armillaria* is rich in nutritional and functional compounds (Wu et al. 2012; Chen et al. 2014). For example, sesquiterpenoids are the characteristic components of *Armillaria*, with bioactivities of immunomodulation and anti-tumour (Misiak et al.

2009; Bohnert et al. 2014); polysaccharides are the main material basis for the bioactivities of *Armillaria*, with the function of liver-protection, hypoglycaemic, and anti-oxidation (Sun et al. 2009); adenosines are highly correlated with energy metabolism and physiological regulation, such as arrhythmias prevention and improvement of blood circulation (Watanabe et al. 1990).

Antagonism between co-cultured mycelia of different fungal species has been widely observed (Barbosa et al. 2001; Raziq and Fox 2003; Qualhato et al. 2013). The mechanisms underlying fungal antagonism often include nutrient and space competition, and the production of antifungal metabolites (Gloer 1995; Heilmann-Clausen and Boddy 2005; Peay et al. 2008; Lorito et al. 2010). For example, abundant antifungal metabolites such as caffeic acid and eugenol were identified from the co-cultured liquid media of *Leclercia adecarboxylata* WT16 and *Aspergillus flavus*

CONTACT Fuqiang Yu  fqyu@mail.kib.ac.cn; Yanliang Wang  wangyanliang@mail.kib.ac.cn

[#]co-first authors

 Supplemental data for this article can be accessed online at <https://doi.org/10.1080/21501203.2023.2238753>

© 2023 The Author(s). Published by Informa UK Limited, trading as Taylor & Francis Group.

This is an Open Access article distributed under the terms of the Creative Commons Attribution-NonCommercial License (<http://creativecommons.org/licenses/by-nc/4.0/>), which permits unrestricted non-commercial use, distribution, and reproduction in any medium, provided the original work is properly cited. The terms on which this article has been published allow the posting of the Accepted Manuscript in a repository by the author(s) or with their consent.

(Xie et al. 2021); 1*H*-pyrrole-2-carboxylic acid that separated from the metabolites of *Streptomyces griseus* exerted strong antagonistic effect on *Phytophthora capsici* (Nguyen et al. 2015); volatile organic compounds including monoterpene eucalyptol and 1,8-cineol produced by *Nodulisporium* sp. GS4d2II1a showed antifungal activities against *Aspergillus parasiticus*, *Aspergillus niger*, and *Sclerotinia sclerotiorum* (Sanchez-Fernandez et al. 2016). Furthermore, the mycelial growth of certain species could be significantly inhibited when the antagonism occurred (Anith et al. 2021; Rajani et al. 2021; Hyder et al. 2022). The confrontation culture experiment (Mallett and Hiratsuka 1986; Hopkin et al. 1989) indicated that there was usually an interspecific black antagonistic line at the site of contact between two colonies of different *Armillaria* biological species. Currently, studies on the metabolic composition of *Armillaria* primarily focused on the mycelia of *Armillaria* cultured separately or their fruiting bodies (Yang et al. 1989; Donnelly et al. 1997; Cremin et al. 2000). It is unclear how the metabolic changes in response to co-culture of different *Armillaria* biological species with antagonism zones.

Metabolomics analysis has been widely used in pharmacology, biology, and many other research fields to accurately reflect the physiological responses of organisms to biotic and abiotic stimuli (Seo and Shin 2022). Various metabolomics analysis strategies have their own advantages and application scopes (Saude et al. 2006; Beckonert et al. 2007). Compared to metabolomics analysis strategies such as GC-MS and NMR, LC-MS/MS shows good performance in sensitivity, reproducibility, and coverage of analytes (Plumb et al. 2004; He and Aga 2019). It can greatly improve the separation effect of small-molecule substances, which thus makes it suitable for biomarker identification (t'Kindt et al. 2009; Shi et al. 2021). In this study, two biological species of *Armillaria*, Chinese Biological Species C (C) and Chinese Biological Species G (G) (Qin et al. 2007), were co-cultured (C-G) or cultured separately (C, G) on agar media to see if an antagonistic line could form. Then, they were cultured in liquid media, and the metabolites in the liquid media (mainly mycelial exudates) were analysed by LC-MS/MS to reveal the metabolic responses of *Armillaria* species with antagonism zones. The obtained data will provide a reference for exploring the candidate biomarkers and the key metabolic pathways involved in *Armillaria* antagonist.

2. Materials and methods

2.1. Experimental materials

Two biological species of *Armillaria* from the study of Qin et al. (2007) were used in this study: Chinese Biological Species C (C), which was collected from Changbai Mountain in Jilin Province; Chinese Biological Species G (G), which was collected from Taiwan Province.

2.2. Experimental design

An antagonistic experiment on agar media was conducted as follows: mycelia of C and G were cultured on PDA media (200 g potato, 20 g glucose, and 20 g agar in 1,000 mL water), respectively, for 15 days firstly. Then, punches with a diameter of 1 cm were used to transfer mycelia to new PDA media under three culture modes: C-G co-culture, C and G separate culture, with at least three replicates. Two mycelial plugs were placed on each plate with a distance of 3 cm, and the antagonism zones between colonies were observed after incubation at 25 °C in the dark for 45 days.

The co-culture experiment in liquid media was conducted as follows: mycelia of C and G were cultured on PDA media, respectively, for 15 days. Subsequently, a total of 20 mycelia plugs were transferred to 300 mL of MYA liquid media (20 g malt extract, 5 g yeast extract, 30 g sucrose, and 13 g agar in 1,000 mL water) under the same three culture modes (C-G co-culture, C and G separate cultures), with four replicates. The flasks were incubated in the dark at 25 °C, shaking at 100 r/min in the first week, then were placed under static conditions but were shaken for 30 s manually every 2 days. After 45 days, the flasks were slightly shaken to mix homogeneously and 10 mL of culture solution from each flask was sampled for filtration, and the filtrate was frozen with liquid nitrogen and stored at -80 °C until metabolome analysis.

2.3. Metabolomics analysis

2.3.1. Metabolites extraction

The liquid samples (1 mL) were freeze-dried, added with 100 µL of precooled ethanol/acetonitrile/water solution (2:2:1, v/v/v), vortex mixed, low-temperature ultra-sounded for 30 min, stayed at -20 °C for 10 min, 14,000 ×g, 4 °C for 20 min. The supernatant was further vacuum dried and added to

100 μ L of acetonitrile aqueous solution (acetonitrile: water = 1:1, v/v), following vortexing, samples were then centrifuged (14,000 $\times g$) at 4 °C for 15 min, and the supernatant was used for subsequent analysis.

2.3.2. Chromatographic conditions

The samples were separated by HILIC column of ultra-high performance liquid chromatography, with column temperature at 40 °C, flow rate of 0.4 mL/min, and injection volume of 2 μ L. Mobile phase A: water, 25 mmol/L of ammonium acetate, and 25 mmol/L of ammonia; mobile phase B: acetonitrile. The gradient elution procedure was set as 95% B for 0–0.5 min; B changed linearly from 95% to 65% within 7 min, then from 65% to 40% within 8 min, and maintained at 40% for 8–9 min; subsequently changed linearly from 40% to 95% within 9 min, and maintained at 95% for 9–12 min (Yang et al. 2020).

2.3.3. Q-TOF mass spectrometry conditions

The ESI source conditions were set in according to Yang et al. (2020): ion source gas I 50, ion source gas II 50, curtain gas 30, source temperature of 500 °C, $\pm 5,500$ V for ion spray voltage floating in the negative and positive ion modes. The product ion scan was acquired using information-dependent acquisition (IDA) with high-sensitivity mode. The collision energy was fixed at 35 ± 15 eV, and ± 80 V for declustering potential in the negative and positive ion modes.

2.4. Data processing

The raw MS data (wiff.scan files) were converted to .mzXML files using ProteoWizard MSConvert (Shen et al. 2016). Peak alignment, retention time correction, and peak area extraction were performed by XCMS. CAMERA (Collection of Algorithms of METabolite pRofile Annotation) was used for annotation of isotopes and adducts. Compound identification of metabolites was performed by comparing accuracy m/z value (<10%), and MS/MS spectra with databases of mzCloud (www.mzcloud.org/), mzVault, and Masslist.

2.5. Statistics analysis

After normalised to total peak intensity, the processed data were analysed by SIMCA 14.1 and Origin 2022, where it was subjected to multivariate data analysis,

including Pareto-scaled principal component analysis (PCA) and orthogonal partial least-squares discriminant analysis (OPLS-DA). The VIP (variable importance in the projection) value of each variable in the OPLS-DA model together with the Student's *t*-test was performed to screen significantly differentially expressed metabolites (VIP value > 1, FC > 1.2 or FC < 0.833, and *P* value < 0.05). The differentially expressed metabolites were then qualitatively hierarchical clustered and submitted to KEGG (www.genome.jp/kegg/) and MetaboAnalyst (www.metaboanalyst.ca/) for metabolic pathway analysis.

3. Results

3.1. Antagonism zone between *Armillaria C* and *G*

When *Armillaria* species of C and G were paired in culture on agar medium, an antagonistic line was observed at the confronting margins of the colonies, but not when the same species were cultured separately. Moreover, the mycelial growth of C was likely inhibited in the co-culture plate (Figure 1).

3.2. Overview of metabolome analysis

Quality control analysis showed that the response strength and retention time of each chromatographic peak of QC samples basically overlapped, and the correlation coefficients were all higher than 0.9, indicating that the experimental process was stable and reliable (Figure S1). A total of 741 metabolites in the negative ion mode and 1,636 metabolites in the positive ion mode were identified (Table S1). These metabolites were classified into 18 superclasses, mainly including 709 organic acids and derivatives, 348 lipids and lipid-like molecules, 292 organoheterocyclic compounds, etc. (Figure 2). PCA analysis could define the differences among the three culture modes, where PC1 explained more than 43% of the variance for modelling. However, some overlap in the samples could be seen and high variation within the samples of the same culture mode could be observed [Figure S2(a,c)]. After filtering out the orthogonal variables irrelevant to categorical variables, OPLS-DA analysis could nicely define the differences among these three culture modes [Figure S2(b,d)]. These results suggested that the C-G co-cultured mode had significantly different metabolic characteristics, compared to their separate culture modes.

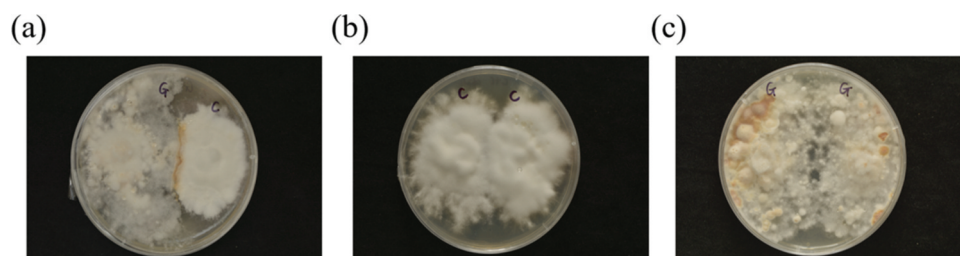


Figure 1. Observation of antagonistic zone of different species of *Armillaria*. (a) C and G paired in culture on agar medium. (b) C and C paired in culture on agar medium. (c) G and G paired in culture on agar medium.

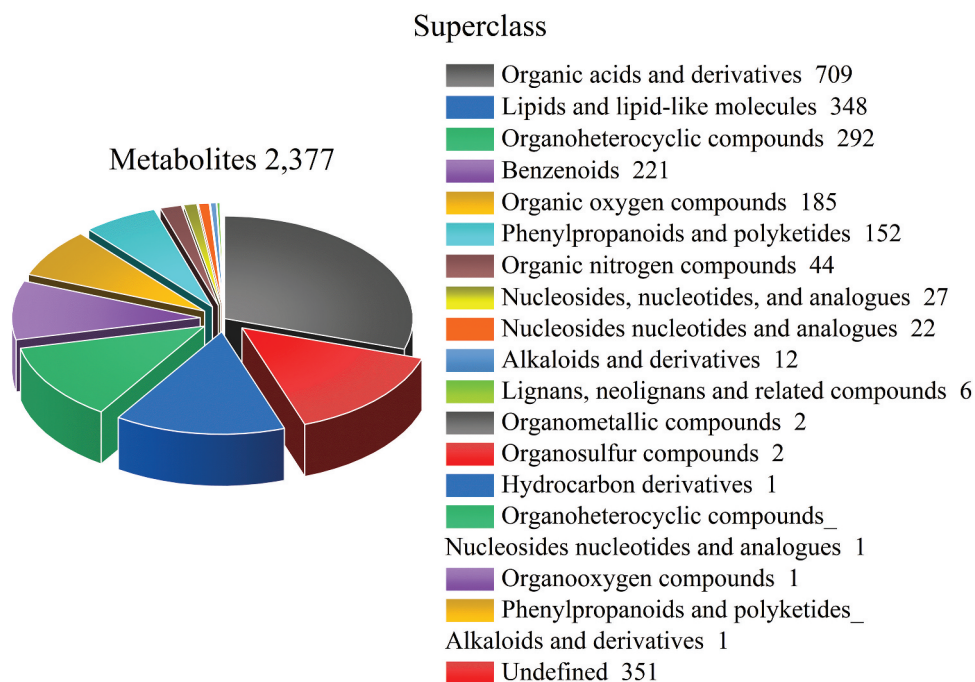


Figure 2. Superclasses of the identified metabolites.

3.3. Differentially expressed metabolites induced by co-culture of C and G

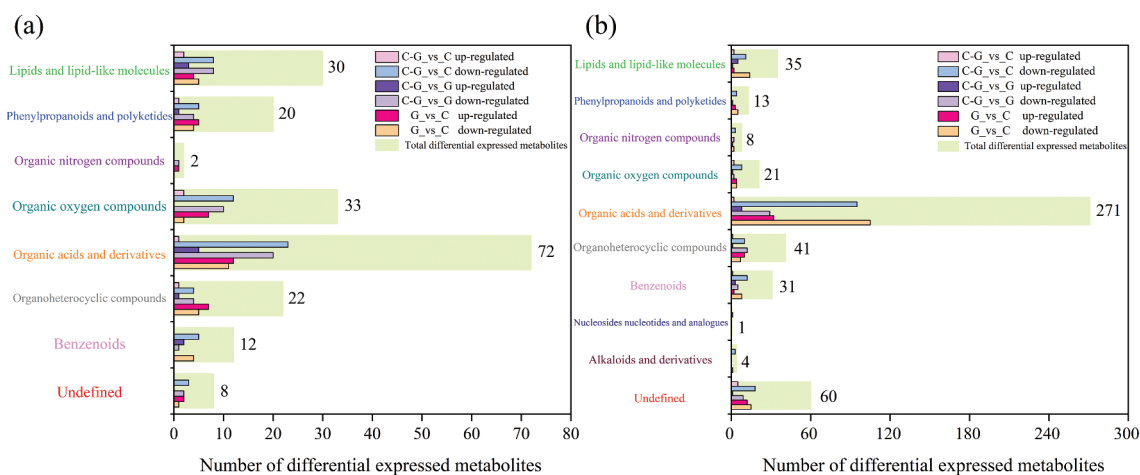
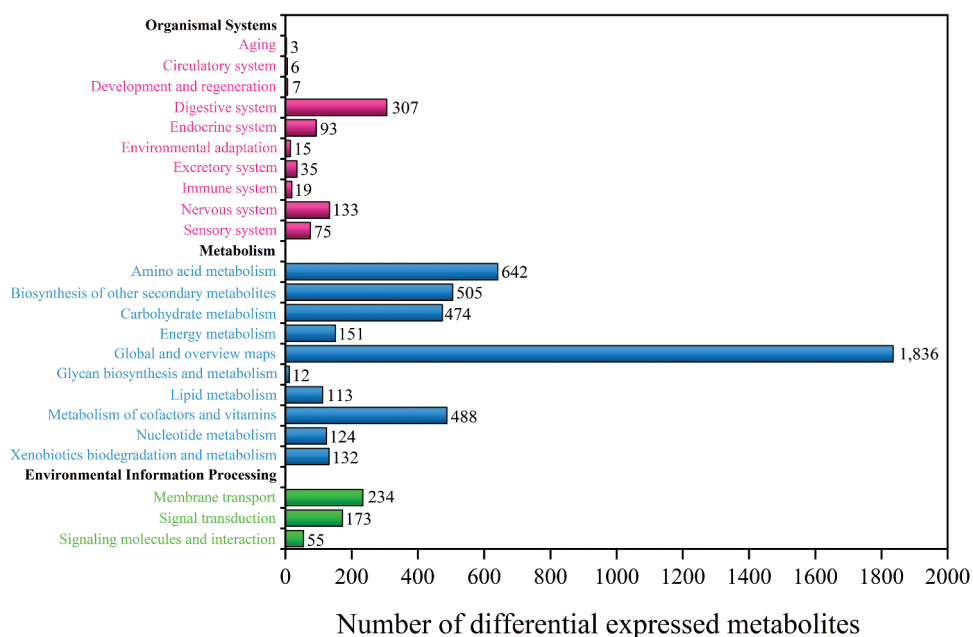
There were a total of 248 differentially expressed metabolites (20 up-regulated and 228 down-regulated) between group C-G and C, 142 differentially expressed metabolites (31 up-regulated and 111 down-regulated) between group C-G and G, and 297 (104 up-regulated and 193 down-regulated) between group G and C (Tables 1, S2, and S3). Among these differentially expressed metabolites, the largest number of metabolites belonged to organic acids and derivatives (343), followed by lipids and lipid-like molecules (65), and organoheterocyclic compounds (63) (Figure 3). The differentially expressed metabolites were categorised into three major metabolic pathways: organismal systems,

metabolism, and environmental information processing, with the largest number of metabolites, were categorised into metabolism pathway. Within the metabolism pathway, 1,836 metabolites were categorised into global and overview maps (Figure 4).

Wayne analysis found 14 common differentially expressed metabolites among the three culture modes in the negative and positive ion modes: lithosprmoside, (+)-.gamma.-tocopherol, Glu-His, malate, Leu-Arg, uracil, 2-chloro-2"-hydroxy-4"-methylbenzophenone, His-His-Arg, 4-hydroxyquinoline, cucurbitacin i, arenobufagin, Leu-Gln-Arg, 4-piperidinecarboxamide, and physcion [Figure 5(a, c)]. Hierarchical clustering analysis showed that the samples of each culture mode were clustered together, indicating that metabolic characteristics

Table 1. Quantitative statistics of differentially expressed metabolites.

Comparison groups	Number of differentially expressed metabolites	Up-regulated metabolites	Down-regulated metabolites
C-G vs C neg	67	7	60
C-G vs C pos	181	13	168
C-G vs G neg	62	12	50
C-G vs G pos	80	19	61
G vs C neg	70	38	32
G vs C pos	227	66	161

**Figure 3.** Number of differentially expressed metabolites in different superclasses in the negative (a) and positive (b) ion modes, respectively. Different superclasses in y axis are distinguished with different colours.**Figure 4.** KEGG pathways for the differentially expressed metabolites.

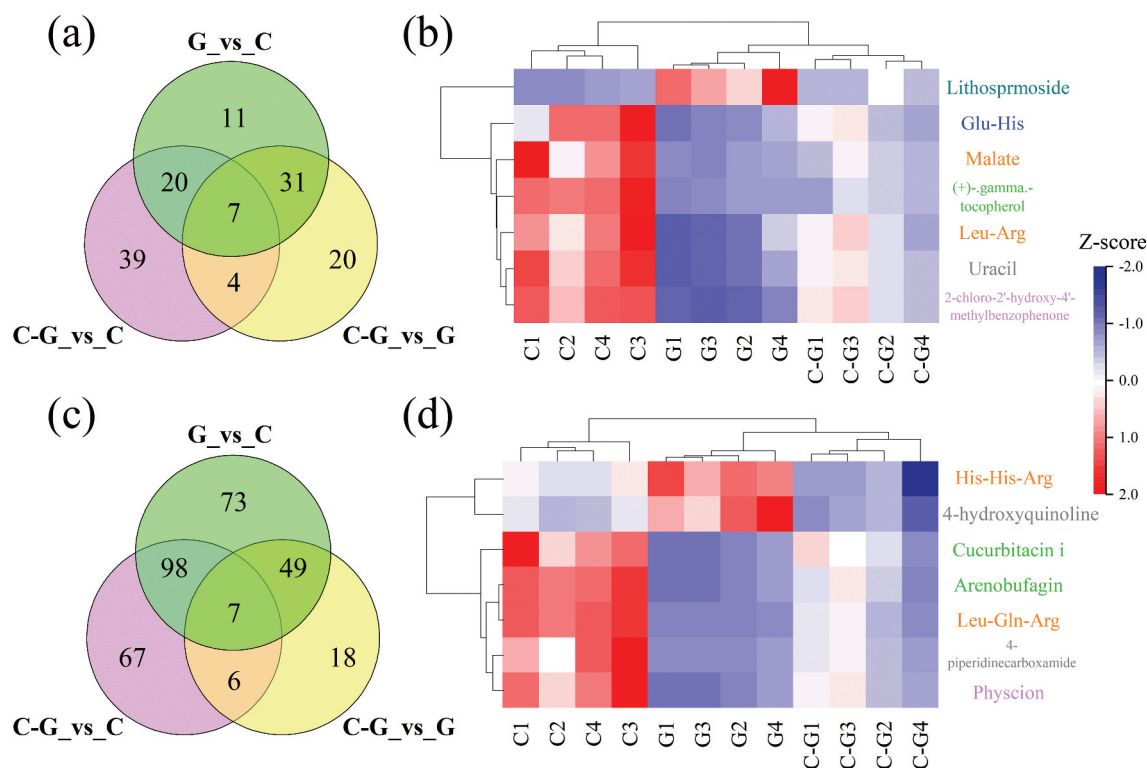


Figure 5. (a), (c) Venn diagrams of differentially expressed metabolites among the comparison groups in the negative and positive ion modes, respectively. (b), (d) Cluster heat maps of common differentially expressed metabolites in the negative and positive ion modes, respectively. The colour bar in heat maps indicates the content levels (represented as the transformed intensity of original peak); red indicates the high content level and blue indicates low content level. Numbers on the axis represent Z-score, $Z=(x-\mu)/\sigma$; x represents the intensity of original peak; μ represents average; σ represents standard deviation. The colours of the differentially expressed metabolites in y axis correspond to the colours of superclasses in Figure 3, the same colour represents the affiliation. Same below.

in the same group were similar. Eleven of the 14 common differentially expressed metabolites (except lithosprmoside, his-his-arg, and 4-hydroxyquinoline) were generally greater in the culture solution of C than G and were repressed in co-culture mode C-G [Figure 5(b,d) and Figure S3].

KEGG topology analysis showed a total of 29 significantly enriched metabolic pathways in group C-G versus C. Based on the P values, the top five metabolic pathways were protein digestion and absorption, ABC transporters, aminoacyl-tRNA biosynthesis, mineral absorption, and biosynthesis of amino acids (Figure 6a, Table S4). In group C-G versus G, 25 metabolic pathways were enriched significantly, with the top five metabolic pathways were: TCA cycle, carbon fixation pathways in prokaryotes, pyruvate metabolism, taste transduction, glyoxylate, and dicarboxylate metabolism (Figure 6b, Table S5). Among these metabolic pathways, TCA cycle, taste transduction, glyoxylate and dicarboxylate metabolism,

pyrimidine metabolism, carbohydrate digestion and absorption, and mineral absorption were overlapped between these two comparison groups. Common differentially expressed metabolites and categorised metabolic pathways, malate and TCA cycle, as well as uracil and pyrimidine metabolism, were highly correlated, which could be speculated as the candidate biomarkers and the key metabolic pathways involved in fungal antagonists of *Armillaria*.

3.4. New metabolites induced by co-culture of *Armillaria C* and *G*

Compared to the separate culture modes, a total of 156 new metabolites induced by C-G co-culture were identified, which were classified into nine superclasses (Figure 7). These new metabolites covered 80 metabolic pathways, and 15 new metabolites were categorised into the biosynthesis of secondary metabolites. Among these new metabolites, 32 potential

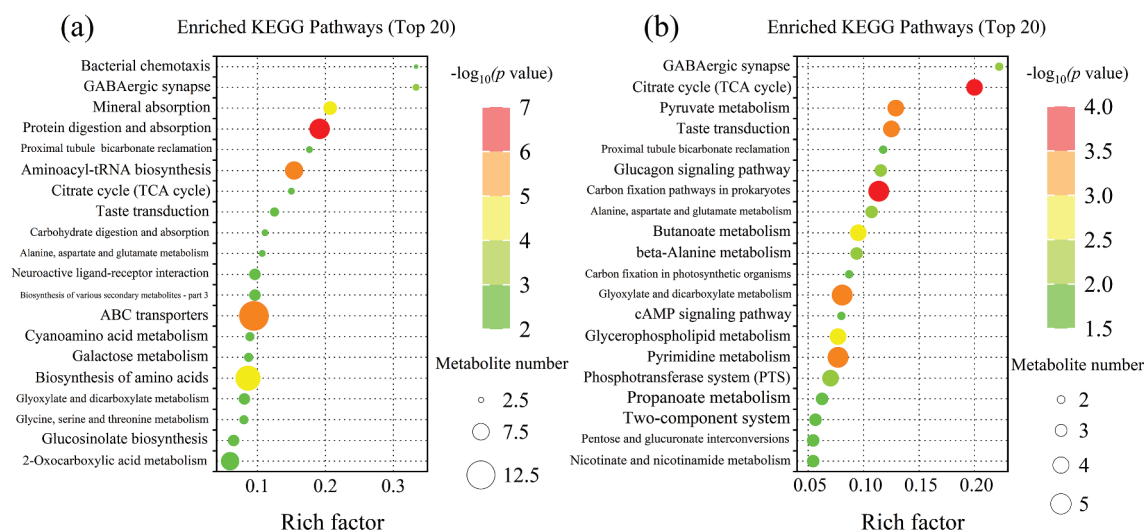


Figure 6. KEGG pathways of differentially expressed metabolites in group C-G versus C (a) and group C-G versus G (b), respectively. In the bubble diagram, each bubble represents a metabolic pathway (top 20 with significance).

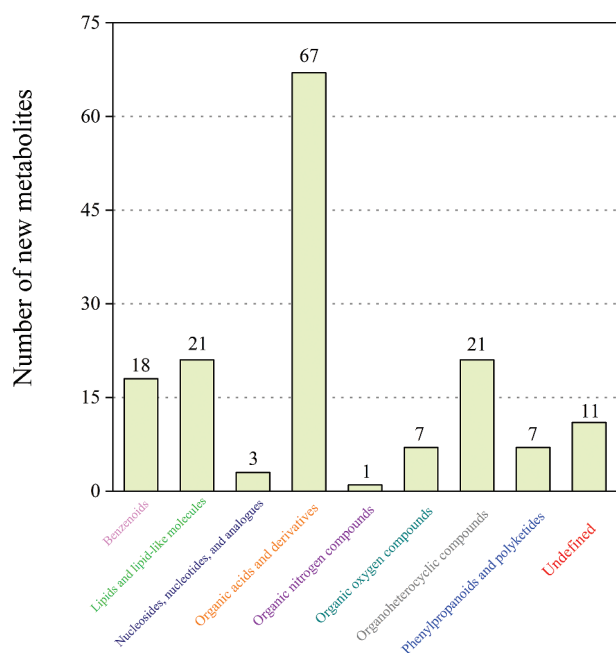


Figure 7. Superclasses of the new metabolites induced by C-G culture.

antifungal metabolites were found, primarily enriched into organic acids and derivatives (10 metabolites) (Table S6).

4. Discussion

Numerous studies on the chemical components of *Armillaria* mycelia cultured separately or their fruiting bodies have been reported from the late 1970s, and

compounds like protoilludane sesquiterpenoids, polysaccharides, sterols, etc. were rich in *Armillaria* (Obuchi et al. 1990; Momose et al. 2000; Puzyr et al. 2017; Li et al. 2020a; Erbiai et al. 2021). In this study, a large number of metabolites (709) belonging to organic acids and derivatives were identified from mycelial exudates and differentially expressed metabolites belonging to organic acids and derivatives changed mostly among different culture modes, indicating that organic acids and derivatives were the dominant components in mycelial exudates of *Armillaria*. Sixteen metabolites belonging to sesquiterpenoids were identified, but they were not significantly affected by co-culture mode. Moreover, metabolites like lignans, neolignans, and polyketides were identified in our study, but were rarely identified from the mycelia and fruiting bodies in previous studies (Muszynska et al. 2011; Zhang et al. 2015; Li et al. 2016; Ren et al. 2022), showing the metabolic differences between mycelial exudates, mycelia and fruiting bodies. Furthermore, compared to the separate culture modes, polyketides were generally repressed in C-G co-culture, which might be due to metabolic changes in response to biotic stimulus in the co-culture of *Armillaria* species with antagonism effect (Nicoletti et al. 2004; Arredondo-Santoyo et al. 2018; Dullah et al. 2021). Lignans and neolignans, which were newly identified in our study, had significant bioactivities: lignans could inhibit the formation and growth of hormone-dependent cancer cells and protect the human body against oestrogen-related

diseases, such as osteoporosis and breast cancer (lonkova 2011). Polyketides, which could be isolated from the co-culture of *Armillaria* and *Phoma* sp. YUD17001 showed bioactivities of antibacterial, anti-parasitic, anticancer, hypolipidemic, and immunosuppressant (Das and Khosla 2009; Li et al. 2020b).

Common differentially expressed metabolites can be used as the candidate biomarkers (Kalantari et al. 2019; Shi et al. 2021). In this study, common differentially expressed metabolites malate and common categorised metabolic pathways TCA cycle showed high correlation, thus could be speculated as the candidate biomarker and key metabolic pathway involved in interspecies antagonism of *Armillaria*. Malate can be an antibacterial substance and can induce chemotaxis and biofilm formation of antagonistic bacteria specifically (Jog et al. 2014; Wang et al. 2021). Organic acids including malate are the intermediate products of the TCA cycle, which can affect TCA cycle as energy and/or signal substances (Goldberg et al. 2006). Compared with group C and G, 91.3% of organic acids and derivatives were significantly repressed in group C-G, suggesting that the TCA cycle might be inhibited or blocked (Raimundo et al. 2011), and hereby restricted mycelial growth in the co-culture mode. Uracil, as an important component of pyrimidine metabolism (commonly categorised metabolic pathways), could be used as another candidate biomarker in our study. Uracil auxotrophic mutants of *Pichia anomala* strain K showed inferior antagonism and colonisation activities (Grevesse et al. 2003).

A total of 70 enriched metabolic pathways overlapped between group C-G versus C (119 metabolic pathways) and group C-G versus G (86 metabolic pathways), suggesting that C and G might have similar metabolic characteristics. However, the most significantly enriched metabolic pathways were exclusive between the comparison groups when C and G were paired in culture, which indicated that significantly differentially metabolic characteristics might be produced by C-G co-culture. In this study, a total of 156 new metabolites were induced by the co-culture of C and G, and 32 metabolites with potentially antifungal activities. Leucine, an antifungal metabolite belonging to organic acids, was separated from the fermentation broth of an unidentified fungus (Hedge et al. 2001). In the composition of

differentially expressed metabolites, new metabolites, and antifungal metabolites induced by C-G co-culture, the number of organic acids and derivatives was the largest, indicating that organic acids and derivatives might affect some metabolic pathways involved in fungal antagonists of *Armillaria* (Hirozawa et al. 2023). 2,4-di-tert-butylphenol, an antifungal secondary metabolite produced by *Aspergillus flavus* YRB2, exhibited strong antagonistic activity against *Fusarium solani* *in vitro* (Rashad et al. 2022). In this study, the new metabolites induced by C-G co-culture were mostly enriched into the biosynthesis of secondary metabolites. It might be correlated with the mechanisms involved in antagonism between different *Armillaria* biological species, which need further study. Thymine isolated from *Penicillium chrysogenum* sp. ZZ1151 showed antimicrobial activity against *Escherichia coli* and *Candida albicans* (Newaz et al. 2022). Furthermore, thymine was an important component of pyrimidine metabolism, which was speculated as the key metabolic pathway involved in fungal antagonists of *Armillaria* in our study. These results on metabolites from *Armillaria* antagonists could enrich our understanding of the metabolic responses of *Armillaria* species with antagonism zones and help to discover antifungal metabolites, the candidate biomarkers, and the key metabolic pathways involved in metabolic mechanisms underlying fungal antagonists of *Armillaria*, which provided references for its potential application as a biocontrol agent.

The content of fungal metabolites shall be related to the mycelial biomass. The biomass of mycelia was not measured in the current study due to the presence of agar on mycelia and the difficulty in collecting all mycelium in a liquid culture system. The mycelial growth of *Armillaria* C in the co-culture mode might be negatively affected. However, the same number of mycelia-containing agar plugs with the same diameter were put into each flask, making the data still comparable and the results might still reflect the relative differences among different culture modes. Furthermore, the targeted metabolomics analysis shall be used to verify the findings in this study, and the activities and functions of differentially expressed metabolites, as well as the new metabolites induced by co-culture mode need further study.

5. Conclusion

This study analysed metabolites in the mycelium culture solution of *Armillaria* species with an antagonistic line. We found that the contents of organic acids and derivatives in the culture solutions changed greatly, and some new metabolites were produced in the co-culture mode. Furthermore, malate and uracil could be used as the candidate biomarkers, and TCA cycle and pyrimidine metabolism might be the key metabolic pathways involved in fungal antagonists of *Armillaria*.

Acknowledgments

We thank Guofu Qin (Liaoning Red Cross) for providing *Armillaria* isolates, Rui Chen (Shaanxi Normal University) for the pre-culture of *Armillaria* mycelia, and Prof. Xinhua He (Southwest University) for linguistic correction.

Disclosure statement

No potential conflict of interest was reported by the author(s).

Funding

This work was supported by the Kunming Institute of Botany, Chinese Academy of Sciences (Y9627111K1); the Yunnan High Level Talent Introduction Plan (YNQR-QNRC-2019-057); the Yunnan Province Science and Technology Department (E2313442).

ORCID

Yanliang Wang  <http://orcid.org/0000-0001-6095-8235>

Data availability statement

The authors confirm that the data supporting the findings of this study are available within the article and its supplementary materials.

References

Anith KN, Nysanth NS, Natarajan C. 2021. Novel and rapid agar plate methods for *in vitro* assessment of bacterial biocontrol isolates' antagonism against multiple fungal phytopathogens. *Lett Appl Microbiol.* 73(2):229–236. doi: [10.1111/lam.13495](https://doi.org/10.1111/lam.13495).

Arredondo-Santoyo M, Vazquez-Garciduenas MS, Vazquez-Marrufo G. 2018. Identification and characterization of the biotechnological potential of a wild strain of

Paraconiothyrium sp. *Biotechnol Progr.* 34(4):846–857. doi: [10.1002/btpr.2653](https://doi.org/10.1002/btpr.2653).

Barbosa MAG, Rhen KG, Menezes M, Mariano RDLR. 2001. Antagonism of *Trichoderma* species on *Cladosporium herbarum* and their enzymatic characterization. *Braz J Microbiol.* 32(2):98–104. doi: [10.1590/S1517-83822001000200005](https://doi.org/10.1590/S1517-83822001000200005).

Beckonert O, Keun HC, Ebbels TMD, Bundy JG, Holmes E, Lindon JC, Nicholson JK. 2007. Metabolic profiling, metabolomic and metabonomic procedures for NMR spectroscopy of urine, plasma, serum and tissue extracts. *Nat Protoc.* 2(11):2692–2703. doi: [10.1038/nprot.2007.376](https://doi.org/10.1038/nprot.2007.376).

Bohnert M, Mutzmann HW, Schroeckh V, Horn F, Dahse HM, Brakhage AA, Hoffmeister D. 2014. Cytotoxic and antifungal activities of melleolide antibiotics follow dissimilar structure-activity relationships. *Phytochemistry.* 105:101–108. doi: [10.1016/j.phytochem.2014.05.009](https://doi.org/10.1016/j.phytochem.2014.05.009).

Chen YJ, Wu SY, Chen CC, Tsao YL, Hsu NC, Chou YC, Huang HL. 2014. *Armillaria mellea* component *Armillarikin* induces apoptosis in human leukemia cells. *J Funct Foods.* 6:196–204. doi: [10.1016/j.jff.2013.10.007](https://doi.org/10.1016/j.jff.2013.10.007).

Collins C, Keane TM, Turner DJ, O'Keeffe G, Fitzpatrick DA, Doyle S. 2013. Genomic and proteomic dissection of the ubiquitous plant pathogen, *Armillaria mellea*: toward a new infection model system. *J Proteome Res.* 12(6):2552–2570. doi: [10.1021/pr301131t](https://doi.org/10.1021/pr301131t).

Cremin P, Guiry PJ, Wolfender JL, Hostettmann K, Donnelly DMX. 2000. A liquid chromatography–thermospray ionisation–mass spectrometry guided isolation of a new sesquiterpene aryl ester from *Armillaria novae-zelandiae*. *J Chem Soc Perkin Trans 1.* 15(15):2325–2329. doi: [10.1039/b001980l](https://doi.org/10.1039/b001980l).

Das A, Khosla C. 2009. *In vivo* and *in vitro* analysis of the hedamycin polyketide synthase. *Chem Biol.* 16(11):1197–1207. doi: [10.1016/j.chembiol.2009.11.005](https://doi.org/10.1016/j.chembiol.2009.11.005).

Donnelly DMX, Konishi T, Dunne O, Cremin P. 1997. Sesquiterpene aryl esters from *Armillaria tabescens*. *Phytochemistry.* 44(8):1473–1478. doi: [10.1016/S0031-9422\(96\)00599-7](https://doi.org/10.1016/S0031-9422(96)00599-7).

Dullah S, Hazarika DJ, Parveen A, Kakoti M, Borgohain T, Gautom T, Bhattacharyya A, Barooah M, Boro RC. 2021. Fungal interactions induce changes in hyphal morphology and enzyme production. *Mycology.* 12(4):279–295. doi: [10.1080/21501203.2021.1932627](https://doi.org/10.1080/21501203.2021.1932627).

Erbiai E, da Silva LP, Saidi R, Lamrani Z, da Silva JCGE, Maouni A. 2021. Chemical composition, bioactive compounds, and antioxidant activity of two wild edible mushrooms *Armillaria mellea* and *Macrolepiota procera* from two countries (Morocco and Portugal). *Biomolecules.* 11(4):575. doi: [10.3390/biom11040575](https://doi.org/10.3390/biom11040575).

Gloer JB. 1995. The chemistry of fungal antagonism and defense. *Can J Bot.* 73(Suppl.):S1265–S1274. doi: [10.1139/b95-387](https://doi.org/10.1139/b95-387).

Goldberg I, Rokem JS, Pines O. 2006. Organic acids: old metabolites, new themes. *J Chem Technol Biot.* 81(10):1601–1611. doi: [10.1002/jctb.1590](https://doi.org/10.1002/jctb.1590).

Grevesse C, Lepoivre P, Jijakli MH. 2003. Characterization of the exoglucanase-encoding gene *PaEXG2* and study of its role in the biocontrol activity of *Pichia anomala* Strain K. *Phytopathology.* 93(9):1145–1152. doi: [10.1094/PHYTO.2003.93.9.1145](https://doi.org/10.1094/PHYTO.2003.93.9.1145).

- He P, Aga DS. 2019. Comparison of GC-MS/MS and LC-MS/MS for the analysis of hormones and pesticides in surface waters: advantages and pitfalls. *Anal Methods*. 11(11):1436–1448. doi: [10.1039/C8AY02774A](https://doi.org/10.1039/C8AY02774A).
- He W, He P, Aga DS. 2019. Biological species of *Armillariella mellea* in the Greater Xingan mountain and the Changbai mountains in China. *Mycosystema*. 15(1):9–16. doi: [10.13346/j.mycosystema.1996.01.003](https://doi.org/10.13346/j.mycosystema.1996.01.003). Chinese.
- Hedge VR, Silver J, Patel M, Gullo VP, Yarborough R, Huang E, Das PR, Puar MS, Didomenico BJ, Loeberberg D. 2001. Novel fungal metabolites as cell wall active antifungals: Fermentation, isolation, physico-chemical properties, structure and biological activity. *J Antibiot (Tokyo)*. 54(1):74–83. doi: [10.7164/antibiotics.54.74](https://doi.org/10.7164/antibiotics.54.74).
- Heilmann-Clausen J, Boddy L. 2005. Inhibition and stimulation effects in communities of wood decay fungi: Exudates from colonized wood influence growth by other species. *Microb Ecol*. 49(3):399–406. doi: [10.1007/s00248-004-0240-2](https://doi.org/10.1007/s00248-004-0240-2).
- Hirozawa MT, Ono MA, Suguiura IMD, Bordini JG, Ono EYS. 2023. Lactic acid bacteria and *Bacillus* spp. as fungal biological control agents. *J Appl Microbiol*. 134(2):1–12. doi: [10.1093/jambio/ixac083](https://doi.org/10.1093/jambio/ixac083).
- Hopkin AA, Mallett KI, Blenis PV. 1989. The use of L-DOPA to enhance visualization of the “black line” between species of the *Armillaria mellea* complex. *Can J Bot*. 67(1):15–17. doi: [10.1139/b89-002](https://doi.org/10.1139/b89-002).
- Hyder S, Gondal AS, Rizvi ZF, Iqbal R, Hannan A, Sahi ST. 2022. Antagonism of selected fungal species against *Macrophomina phaseolina* (tassi) gold, causing charcoal rot of mungbean. *Pak J Bot*. 54(3):1129–1138. doi: [10.30848/PJB2022-3\(8\)](https://doi.org/10.30848/PJB2022-3(8)).
- Ionkova I. 2011. Anticancer Lignans-from discovery to biotechnology. *Mini Rev Med Chem*. 11(10):843–856. doi: [10.2174/138955711796575425](https://doi.org/10.2174/138955711796575425).
- Jog R, Pandya M, Nareshkumar G, Rajkumar S. 2014. Mechanism of phosphate solubilization and antifungal activity of *Streptomyces* spp. isolated from wheat roots and rhizosphere and their application in improving plant growth. *Microbiol Sgm*. 160:778–788. doi: [10.1099/mic.0.074146-0](https://doi.org/10.1099/mic.0.074146-0).
- Kalantari S, Chashmian S, Nafar M, Zakeri Z, Parvin M. 2019. Metabolomics approach reveals urine biomarkers and pathways associated with the pathogenesis of lupus nephritis. *Iran J Basic Med Sci*. 22(11):1288–1295. doi: [10.22038/ijbms.2019.38713.9178](https://doi.org/10.22038/ijbms.2019.38713.9178).
- Korhonen K. 1978. Interfertility and clonal size in the *Armillaria mellea* complex. *Karstenia*. 18(2):31–42. doi: [10.29203/ka.1978.135](https://doi.org/10.29203/ka.1978.135).
- Li HT, Tang LH, Liu T, Yang RN, Yang YB, Zhou H, Ding ZT. 2020a. Protoilludane-type sesquiterpenoids from *Armillaria* sp. by co-culture with the endophytic fungus *Epicoccum* sp. associated with *Gastrodia elata*. *Bioorg Chem*. 95:103503. doi: [10.1016/j.bioorg.2019.103503](https://doi.org/10.1016/j.bioorg.2019.103503).
- Li HT, Liu T, Yang RN, Xie F, Yang Z, Yang YB, Zhou H, Ding ZT. 2020b. Phomretones A-F, C₁₂ polyketides from the co-cultivation of *Phoma* sp. YUD17001 and *Armillaria* sp. *RSC Adv*. 10(31):18384–18389. doi: [10.1039/D0RA02524K](https://doi.org/10.1039/D0RA02524K).
- Li ZJ, Wang YC, Jiang B, Li WL, Zheng LH, Yang XG, Bao YL, Sun LG, Huang YX, Li YX. 2016. Structure, cytotoxic activity and mechanism of protoilludane sesquiterpene aryl esters from the mycelium of *Armillaria mellea*. *J Ethnopharmacol*. 184:119–127. doi: [10.1016/j.jep.2016.02.044](https://doi.org/10.1016/j.jep.2016.02.044).
- Lorito M, Woo SL, Harman GE, Monte E. 2010. Translational Research on *Trichoderma* from ‘Omics to the Field. *Annu Rev Phytopathol*. 48(1):395–417. doi: [10.1146/annurev-phyto-073009-114314](https://doi.org/10.1146/annurev-phyto-073009-114314).
- Mallett KI, Hiratsuka Y. 1986. Nature of the “black line” produced between different biological species of the *Armillaria mellea* complex. *Can J Bot*. 64(11):2588–2590. doi: [10.1139/b86-342](https://doi.org/10.1139/b86-342).
- Matheny PB, Curtis JM, Hofstetter V, Aime MC, Moncalvo JM, Ge ZW, Yang ZL, Slot JC, Ammirati JF, Baroni TJ, et al. 2006. Major clades of Agaricales: a multilocus phylogenetic overview. *Mycologia*. 98(6):982–995. doi: [10.1080/15572536.2006.11832627](https://doi.org/10.1080/15572536.2006.11832627).
- Misiek M, Williams J, Schmich K, Huttel W, Merfort I, Salomon CE, Aldrich CC, Hoffmeister D. 2009. Structure and cytotoxicity of arnamial and related fungal sesquiterpene aryl esters. *J Nat Prod*. 72(10):1888–1891. doi: [10.1021/np900314p](https://doi.org/10.1021/np900314p).
- Momose I, Sekizawa R, Hosokawa N, Iinuma H, Maisui S, Nakamura H, Naganawa H, Hamada M, Takeuchi T. 2000. Melleolides K, L and M, new melleolides from *Armillariella mellea*. *J Antibiot (Tokyo)*. 53(2):137–143. doi: [10.7164/antibiotics.53.137](https://doi.org/10.7164/antibiotics.53.137).
- Muszynska B, Sulkowska-Ziajka K, Wolkowska M, Ekiert H. 2011. Chemical, pharmacological, and biological characterization of the culinary-medicinal honey mushroom, *Armillaria mellea* (Vahl) P. Kumm. (Agaricomycetidae): A review. *Int J Med Mushrooms*. 13(2):167–175. doi: [10.1615/IntJMedMushr.v13.i2.90](https://doi.org/10.1615/IntJMedMushr.v13.i2.90).
- Newaz AW, Yong K, Yi WW, Wu B, Zhang ZZ. 2022. Antimicrobial metabolites from the Indonesian mangrove sediment-derived fungus *Penicillium chrysogenum* sp. ZZ1151. *Nat Prod Res*. 37(10):1702–1708. doi: [10.1080/14786419.2022.2103813](https://doi.org/10.1080/14786419.2022.2103813).
- Nguyen XH, Naing KW, Lee YS, Kim YH, Moon JH, Kim KY. 2015. Antagonism of antifungal metabolites from *Streptomyces griseus* H7602 against *Phytophthora capsici*. *J Basic Microbiol*. 55(1):45–53. doi: [10.1002/jobm.201300820](https://doi.org/10.1002/jobm.201300820).
- Nicoletti R, De Stefano M, De Stefano S, Trincone A, Marziano F. 2004. Antagonism against *Rhizoctonia solani* and fungitoxic metabolite production by some *Penicillium* isolates. *Mycopathologia*. 158(4):465–474. doi: [10.1007/s11046-004-3712-5](https://doi.org/10.1007/s11046-004-3712-5).
- Obuchi T, Kondoh H, Watanabe N, Tamai M, Imura S, Yang JS, Liang XT. 1990. Armillaric acid, a new antibiotic produced by *Armillaria mellea*. *Planta Med*. 56(2):198–201. doi: [10.1055/s-2006-960925](https://doi.org/10.1055/s-2006-960925).
- Peay KG, Kennedy PG, Bruns TD. 2008. Fungal community ecology: A hybrid beast with a molecular master. *Bioscience*. 58(9):799–810. doi: [10.1641/B580907](https://doi.org/10.1641/B580907).
- Plumb R, Castro-Perez J, Granger J, Beattie I, Joncour K, Wright A. 2004. Ultra-performance liquid chromatography

- coupled to quadrupole-orthogonal time-of-flight mass spectrometry. *Rapid Commun Mass Spectrom.* 18 (19):2331–2337. doi: [10.1002/rcm.1627](https://doi.org/10.1002/rcm.1627).
- Puzyr AP, Medvedeva SE, Bondar VS. 2017. Biochemical changes causes lack of bioluminescence in fruiting bodies of *Armillaria*. *Mycosphere.* 8(1):9–17. doi: [10.5943/mycosphere/8/1/2](https://doi.org/10.5943/mycosphere/8/1/2).
- Qin GF, Zhao J, Korhonen K. 2007. A study on intersterility groups of *Armillaria* in China. *Mycologia.* 99(3):430–441. doi: [10.1080/15572536.2007.11832568](https://doi.org/10.1080/15572536.2007.11832568).
- Qualhato TF, Lopes FAC, Steindorff AS, Brandao RS, Jesuino RSA, Ulhoa CJ. 2013. Mycoparasitism studies of *Trichoderma* species against three phytopathogenic fungi: Evaluation of antagonism and hydrolytic enzyme production. *Biotechnol Lett.* 35(9):1461–1468. doi: [10.1007/s10529-013-1225-3](https://doi.org/10.1007/s10529-013-1225-3).
- Raimundo N, Baysal BE, Shadel GS. 2011. Revisiting the TCA cycle: signaling to tumor formation. *Trends Mol Med.* 17 (11):641–649. doi: [10.1016/j.molmed.2011.06.001](https://doi.org/10.1016/j.molmed.2011.06.001).
- Rajani P, Rajasekaran C, Vasanthakumari MM, Olsson SB, Ravikanth G, Shaanker RU. 2021. Inhibition of plant pathogenic fungi by endophytic *Trichoderma* spp. through mycoparasitism and volatile organic compounds. *Microbiol Res.* 242:126595. doi: [10.1016/j.micres.2020.126595](https://doi.org/10.1016/j.micres.2020.126595).
- Rashad YM, Abdalla SA, Shehata AS. 2022. *Aspergillus flavus* YRB2 from *Thymelaea hirsuta* (L.) Endl., a non-aflatoxigenic endophyte with ability to overexpress defense-related genes against Fusarium root rot of maize. *BMC Microbiol.* 22(1):229. doi: [10.1186/s12866-022-02651-6](https://doi.org/10.1186/s12866-022-02651-6).
- Raziq F, Fox RTV. 2003. Comparisons between the *in vitro* and *in vivo* efficacies of potential fungal antagonists of *Armillaria mellea*. *Biol Agric Hortic.* 21(3):263–276. doi: [10.1080/01448765.2003.9755269](https://doi.org/10.1080/01448765.2003.9755269).
- Ren SZ, Gao YP, Li H, Ma HH, Han XL, Yang ZT, Chen WJ. 2022. Research status and application prospects of the medicinal mushroom *Armillaria mellea*. *Appl Biochem Biotechnol.* 195 (5):3491–3507. doi: [10.1007/s12010-022-04240-9](https://doi.org/10.1007/s12010-022-04240-9).
- Sanchez-Fernandez RE, Diaz D, Duarte G, Lappe-Oliveras P, Sanchez S, Macias-Rubalcava ML. 2016. Antifungal volatile organic compounds from the endophyte *Nodulisporium* sp strain G54d2ll1a: a qualitative change in the intraspecific and interspecific interactions with pythium aphanidermatum. *Microb Ecol.* 71(2):347–364. doi: [10.1007/s00248-015-0679-3](https://doi.org/10.1007/s00248-015-0679-3).
- Saude EJ, Slupsky CM, Sykes BD. 2006. Optimization of NMR analysis of biological fluids for quantitative accuracy. *Metabolomics.* 2(3):113–123. doi: [10.1007/s11306-006-0023-5](https://doi.org/10.1007/s11306-006-0023-5).
- Seo SC, Shin HK. 2022. Simultaneous analysis for quality control of traditional herbal medicine, Gungha-Tang, using liquid chromatography-tandem mass spectrometry. *Molecules.* 27 (4):1223. doi: [10.3390/molecules27041223](https://doi.org/10.3390/molecules27041223).
- Shen XT, Guan XY, Cai YP, Guo Y, Tu J, Li H, Zhang T, Wang JL, Xue FZ, Zhu ZJ. 2016. Normalization and integration of large-scale metabolomics data using support vector regression. *Metabolomics.* 12(5):89. doi: [10.1007/s11306-016-1026-5](https://doi.org/10.1007/s11306-016-1026-5).
- Shi W, Yuan X, Cui KQ, Li H, Fu PH, Rehman SU, Shi DS, Liu QY, Li ZP. 2021. LC-MS/MS based metabolomics reveal candidate biomarkers and metabolic changes in different buffalo species. *Animals.* 11(2):560. doi: [10.3390/ani11020560](https://doi.org/10.3390/ani11020560).
- Sun YX, Liang HT, Zhang XT, Tong HB, Liu JC. 2009. Structural elucidation and immunological activity of a polysaccharide from the fruiting body of *Armillaria mellea*. *Bioresour Technol.* 100(5):1860–1863. doi: [10.1016/j.biortech.2008.09.036](https://doi.org/10.1016/j.biortech.2008.09.036).
- t'Kindt R, Morreel K, Deforce D, Boerjan W, Van Bocxlaer J. 2009. Joint GC-MS and LC-MS platforms for comprehensive plant metabolomics: Repeatability and sample pre-treatment. *J Chromatogr B.* 877(29):3572–3580. doi: [10.1016/j.jchromb.2009.08.041](https://doi.org/10.1016/j.jchromb.2009.08.041).
- Wang Y, Jiang HY, Ma ZW, Wang XM, Li CF, Liu SX. 2021. Screening and identification of antagonistic lactic acid bacteria from fermented coconut water and its antibacterial properties. *Food Res Dev.* 42(23):156–162. doi: [10.12161/j.issn.1005-6521.2021.23.025](https://doi.org/10.12161/j.issn.1005-6521.2021.23.025). Chinese.
- Watanabe N, Obuchi T, Tamai M, Araki H, Omura S, Yang JS, Yu DQ, Liang XT, Huan JH. 1990. A novel N⁶-substituted adenosine isolated from *Armillaria mellea* as a cerebral-protecting compound. *Planta Med.* 56(1):48–52. doi: [10.1055/s-2006-960882](https://doi.org/10.1055/s-2006-960882).
- Wu J, Zhou J, Lang Y, Yao L, Xu H, Shi H, Xu S. 2012. A polysaccharide from *Armillaria mellea* exhibits strong *in vitro* anticancer activity via apoptosis-involved mechanisms. *Int J Biol Macromol.* 51(4):663–667. doi: [10.1016/j.ijbiomac.2012.06.040](https://doi.org/10.1016/j.ijbiomac.2012.06.040).
- Xie HL, Jallow A, Yue XF, Wang XP, Fu JY, Mwakinyali SE, Zhang Q, Li PW. 2021. *Aspergillus flavus*'s response to antagonism bacterial stress sheds light on a regulation and metabolic trade-off mechanism for adversity survival. *J Agric Food Chem.* 69(16):4840–4848. doi: [10.1021/acs.jafc.0c07665](https://doi.org/10.1021/acs.jafc.0c07665).
- Yang JS, Chen YW, Feng XZ, Yu DQ, He CH, Zheng QT, Yang J, Liang XT. 1989. Isolation and structure elucidation of *armillaricin* 1. *Planta Med.* 55(6):564–565. doi: [10.1055/s-2006-962096](https://doi.org/10.1055/s-2006-962096).
- Yang SH, Liu Y, Wang Q, Sun YP, Guan W, Liu Y, Yang BY, Kuang HX. 2020. UPLC-MS/MS identification and quantification of withanolides from six parts of the medicinal plant *Datura metel* L. *Molecules.* 25(6):1260. doi: [10.3390/molecules25061260](https://doi.org/10.3390/molecules25061260).
- Yuan Y, Jin XH, Liu J, Zhao X, Zhou JH, Wang X, Wang DY, Lai CJS, Xu W, Huang JW, et al. 2018. The *Gastrodia elata* genome provides insights into plant adaptation to heterotrophy. *Nat Commun.* 9(1):1615. doi: [10.1038/s41467-018-03423-5](https://doi.org/10.1038/s41467-018-03423-5).
- Zhang SS, Liu XQ, Yan LH, Zhang QW, Zhu JJ, Huang N, Wang ZM. 2015. Chemical compositions and antioxidant activities of polysaccharides from the sporophores and cultured products of *Armillaria mellea*. *Molecules.* 20 (4):5680–5697. doi: [10.3390/molecules20045680](https://doi.org/10.3390/molecules20045680).
- Zhao J, Dai YC, Qin GF. 2008. New biological species of *Armillariella* from China. *Mycosystema.* 27(2):156–170. doi: [10.13346/j.mycosystema.2008.02.007](https://doi.org/10.13346/j.mycosystema.2008.02.007). Chinese.